Melting behavior of ultrathin titanium nanowires

Baolin Wang,[1,2,3,*] Guanghou Wang,[2] Xiaoshuang Chen,[3] and Jijun Zhao[4,†]
[1]*Department of Physics, Huaiyin Teachers College, Jiangsu, 223001, People's Republic of China*
[2]*National Laboratory of Solid State Microstructures and Department of Physics, Nanjing University, Nanjing 210093, People's Republic of China*
[3]*National Laboratory for Infrared Physics, Shanghai Institute of Technical Physics, Chinese Academy of Sciences, Shanghai 200083, People's Republic of China*
[4]*Department of Physics and Astronomy, University of North Carolina at Chapel Hill, North Carolina 27599*
(Received 11 February 2003; published 20 May 2003)

The thermal stability and melting behavior of ultrathin titanium nanowires with multishell cylindrical structures are studied by using empirical molecular-dynamic simulation. The melting temperatures of titanium nanowires show clear dependence on wire sizes and structures. For the nanowire thinner than 1.2 nm, there is no clear characteristic of first-order phase transition during the melting, implying a coexistence of solid and liquid phases due to finite-size effect. An interesting structural transformation from helical multishell cylindrical to bulklike rectangular is observed in the melting process of a thicker nanowire with 1.7 nm diameter.

DOI: 10.1103/PhysRevB.67.193403 PACS number(s): 65.80.+n, 61.46.+w, 68.65.La

Metal nanowires are current focus of intensive research due to both their importance in fundamental low-dimensional physics and the potential applications in nanoscale materials and devices. Experimentally, stable ultrathin metal nanowires with diameter down to several nanometers and sufficient length have been fabricated by various methods.[1–6] For example, Ti nanowires of a few nanometers in width were produced by Ar^+ ions irradiation on Ti thin layer by using carbon nanotube as a mask.[1] Takayanagi's group has successfully produced suspended stable gold wires.[2,3] Novel helical multishell structures are observed in those ultrathin gold and platinum nanowires.[3] The ultrathin metal nanowires are expected to have some unique features different from either bulk solids or nanoclusters because of their larger surface to volume ratio and quantum confinement effect in finite-size systems.

Molecular-dynamics (MD) simulations have been employed to study the structures and properties of free-standing metal nanowires.[7–21] Our group has systematically studied the helical multishell in Au,[14] Ti,[15] Zr (Ref. 16) nanowires based on empirical genetic algorithm simulations. The vibrational, electronic, and transport properties were studied. However, little is known about the thermal stability and melting behavior of such 1D metal nanowires,[7,12,17,22] especially for those ultrathin transition metal nanowires with novel cylindrical multishell structures. For instance, it is important to clarify the dependence of the melting behavior of a metal nanowire on its size and geometries. The finite-size effects,[23–27] e.g., solid-liquid coexistence, on the phase transition of such quasi-1D systems and their evolution with nanowire diameter are also interesting. For thicker crystalline lead nanowires, surface melting effect with the formation of a thin skin of highly mobile surface atoms were observed.[7] More recently, the melting behaviors of the multishell gold nanowires have been also studied by MD simulations.[12,22] In our previous work, the atomic structures of titanium nanowires with diameter from 0.7 to 1.7 nm have been optimized and several representative helical multiwalled cylindrical structures have been obtained.[15] In this Brief Report, we report molecular-dynamic simulations on the thermodynamic properties of the titanium nanowires. The effect of wire sizes and geometries on the melting behavior will be discussed.

In our simulations, Ti nanowires of sufficient length are modeled by supercell with 1D periodical boundary condition along the wire axis direction. As a reasonable compromise between keeping the helicity in *z*-axis direction and avoiding the nanowire breaking into clusters upon relaxation, the length of the supercell is chosen to be 1.256 nm. The interaction between titanium atoms is described by a well-fitted tight-binding many-body potential.[28] To simulate the melting behavior of nanowires, we employ the constant-temperature molecular-dynamics (MD) method by Hoover,[29] which have been extensively used in our previous works.[22,30–32] The MD time step is chosen as 2.15 fs. At each temperature, the initial 10^5 MD steps are used to bring the system into equilibrium. Then we monitor the internal energy E, root-mean-square (rms) fluctuation δ of the interatomic distances, and heat capacity C_v from the thermal statistical averages in the equilibrium canonical ensemble. At each temperature, 10^6 MD steps are performed to record the thermodynamic average of physical properties. The constant-temperature MD simulations start from a low temperature (400 K for nanowires and 200 K for nanoclusters). The temperature gradually increases towards high temperature (1400 K) by 50 K per step.

We have performed comprehensive genetic algorithm simulations on the equilibrium structures of titanium nanowires. The stable multishell structures composed by coaxial cylindrical shells are obtained, which also have been theoretically predicted for Al, Pb, Zr, and Au nanowires[8,14,16] and have been experimentally observed in Au and Pt nanowires.[3] We use index n-n'-n''-n''' to[3,14–16] describe the nanowire consisting of coaxial shells with n, n', n'', n''' helical atomic rows ($n>n'>n''>n'''$) for each shell. Thus the titanium nanowire structures studied (in Table I) can be defined as 8-2, 13-8-2, 9-3, 14-9-3, 9-4, 15-9-4, 5-1, 10-5-1,6-1, 12-6-1, 17-12-6-1, respectively. The structures of the 5-1 and 10-5-1 wires are centered pentagonal sequence containing two-shell,

TABLE I. Overall melting temperatures T_m for titanium nanowires and clusters. The diameter D and number N of atoms in the supercell of the nanowires and clusters are given.

	8-2	13-8-2	9-3	14-9-3	9-4	15-9-4	Ti_{38}	5-1	10-5-1	6-1	12-6-1	17-12-6-1	Ti_{55}	Ti_{147}
N	45	110	57	125	62	138	38	30	80	35	88	169	55	147
D (nm)	0.93	1.43	1.04	1.52	1.07	1.60	1.09	0.75	1.18	0.81	1.28	1.71	1.23	1.81
T_m (K)	800	1050	850	1000	850	950	650	750	900	700	1000	1150	800	900

three-shell with a central single atomic row. The 6-1, 12-6-1, and 17-12-6-1 wires constitute a hexagonal growth sequence containing two-shell, three-shell, and four-shell with a central single atomic row. In contrast, the structures of 8-2 and 13-8-2, 9-3 and 14-9-3, 9-4 and 15-9-4 wires are the three growth sequences without central atomic row. Our systematical illustration of various multishell growth sequences of the metal nanowire can be found elsewhere.[15,16]

Starting from the optimized structures at low temperature, we simulate the melting behavior of the titanium nanowires using constant-temperature MD method. As representative examples, Fig. 1 presents the temperature dependence of the internal energy E, mean-square bond-length fluctuation δ, and thermal capacity C_v for 12-6-1, and 17-12-6-1 nanowires, respectively. From these curves, we can define the overall melting temperature T_m of the system as the temperature at half of saturated δ in liquid states.[22] For the purpose of comparison and discussion, we have also simulated the melting of some titanium nanoclusters with equilibrium structures such as Ti_{38} (truncated octahedron), Ti_{55} (icosahedron), and Ti_{147} (icosahedron), respectively. Table I summarizes the overall melting temperature T_m of various titanium nanowires with different multishell structural patterns from our simulations. In general, the melting temperatures of titanium nanowires are much lower than the experimental bulk melting point (1943 K) and increase with the nanowire size. Because of the 1D periodicity and the well-reconstructed helical surface structures, the melting temperatures of titanium nanowires are typically higher than those of clusters with comparable size (see Table I and Fig. 2).

To explore the size dependence of nanowire melting temperature, we plot the overall melting temperature T_m versus wire diameter $(1/D)$ in Fig. 2. The melting temperatures for several nanoclusters with comparable sizes are also included in Fig. 2 for comparison. The T_m for the 6-1, 12-6-1, 17-12-6-1 wires with the hexagonal growth sequence fit well to a linear dependence as

$$T_m = T_0 - \eta/D,$$

where $T_0 = 1542$ K is the extrapolated melting temperature at the infinite limit, $\eta = 682$ K nm describes the linear dependence of T_m with wire diameter D (in unit of nm). Such $1/D$ dependence of melting temperature for nanowire is similar to the well-known size relationship for metal nanoclusters.[33–35] As compared with the linear size dependence for the hexagonal wires (6-1, 12-6-1, 17-12-6-1), 8-2 and 13-8-2 wires almost belong to the same size relationship while the T_m of other nanowires deviate from such linear fit. These differences indicate that the atomic structures of nanowires play significant role in determining the melting behavior of nanowires. Among these wires, the T_m of 5-1 wire is much higher than the 6-1 wire with a comparable size. On the other hand, the nanowires with three or four atomic strands in the

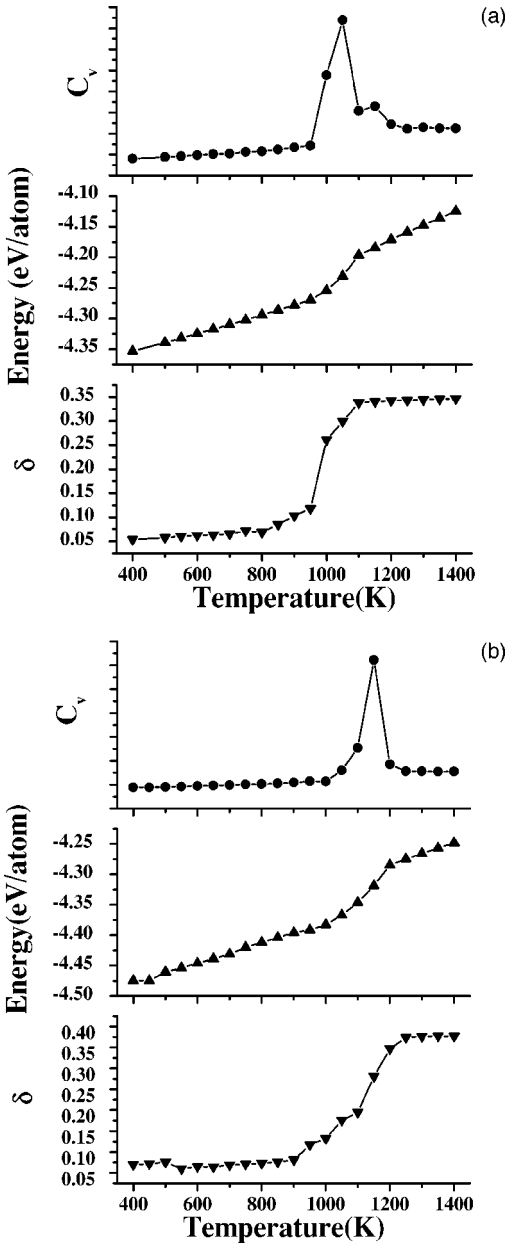

FIG. 1. The rms bond-length fluctuation δ, internal energy E, and heat capacity C_v as functions of temperature for various nanowires: (a) 12-6-1 [upper], (b)17-12-6-1 [lower].

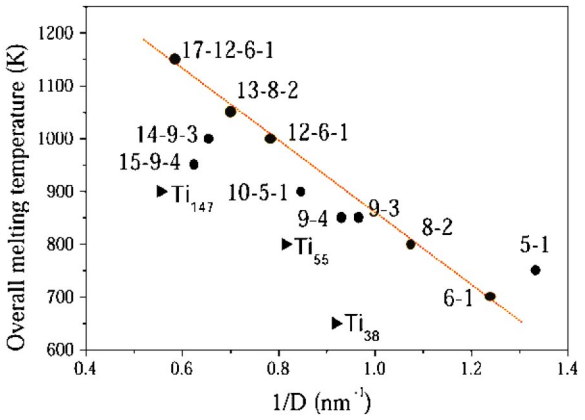

FIG. 2. Overall melting temperature T_m (K) vs nanowire diameters $1/D$(1/nm) for various nanowires with multishell structures. Dashed line is linear fit for hexagonal wires, i.e., 6-1, 12-6-1, 17-12-6-1. The T_m for several nanoclusters are also included.

internal shell such as 9-3, 14-9-3, 9-4, 15-9-4 have lower melting temperature than the nanowires with one atomic strand in the center, e.g., 12-6-1. This effect might be understood by the relatively looser internal structures of these 9-3 or 9-4 based nanowires. Similar results were also found in gold nanowires.[12,22] Therefore, we suggest that the multishell metal nanowires with tight internal structures should have higher thermal stability. Such phenomena are also seen in nanoclusters. For example, the T_m of icosahedral Ti_{55} is much higher than that of Ti_{38} with fcc-like structure. All these results imply that the small transition-metal nanostructures with fivefold symmetry may have relatively higher thermal stability.

We now discuss the detailed melting behavior by examining the temperature dependent curve of internal energy E, bond fluctuation (δ), and thermal capacity (C_v) for various nanowires. The melting of 5-1, 6-1, and 9-4 wires all starts from about 500–600 K. Their differences in the internal structures are only reflected in the slightly different variations of lindemann parameter δ with temperature. In the thinner wires such as 5-1, 6-1, 9-4, we cannot clearly see any peak in the C_v curve, which is a characteristic for the first-order solid to liquid phase transition. Accordingly, the increase of internal energies is also relatively smooth in these small nanowires. Only the rapid jump in bond-length fluctuation with increasing temperature demonstrates the occurrence of melting and evaporation. Similar behavior was found in small clusters.[26] It can be understood by finite-size effect in first-order phase transition,[23,24] which leads to the coexistence of solid and liquid states in a rather broad temperature region.[25–27] On the other hand, the two thicker wires, 12-6-1 and 17-12-6-1, show clear characteristics of the solid to liquid phase transition. In particular, there are sharp peaks in the thermal capacity curves at 1050 K and 1150 K for 12-6-1 and 17-12-6-1 wires, respectively.

In addition to the melting, evaporation may also occur when a solid is heating up. To distinguish melting from evaporation, it is necessary to examine the atomic diffusion and mobility in detail. It is generally thought that when a solid starts melting, the arrangement of the atoms forming

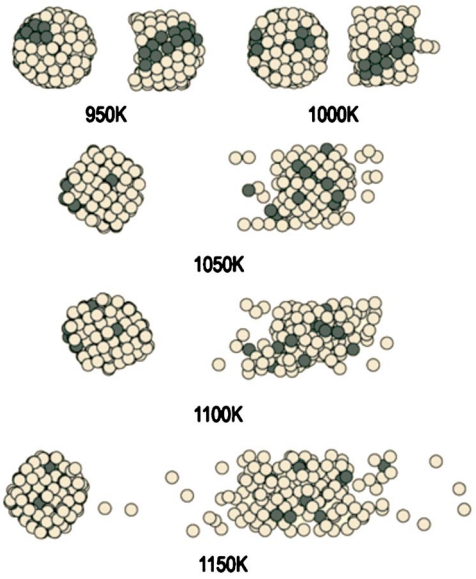

FIG. 3. Snapshot of the 17-12-6-1 nanowire at different temperatures during the melting process. At each temperature, top view (left) and side view (right) of the nanowire structure are given. Several neighboring atoms are marked by black color to trace the motion of atoms.

the solid will become more disordered. Some atoms of the solid will diffuse and mobilize. To further understand the melting process in the titanium nanowires, we have traced the structural change of the 17-12-6-1 wire within the temperatures in the melting region. Figure 3 gives the snapshot of the nanowire at different temperatures. We mark several neighboring atoms, such as surface two atomic strands and several interior-shell atoms, as a target with black color (see Fig. 3). It is found that at 950–1000 K a part of the marked atoms diffuse to other positions. The marked atomic body is broken. Meantime, some relative rotation also occurs for some atoms at the outermost shell. It is thought that the titanium atoms only weakly oscillate at their equilibrium positions at the temperature region. Although there is small deformation on the sharp of nanowire and the diffusion of internal atoms, the top view of the nanowire cross section still shows ''solidlike'' hexagonal structure with three atomic shells. Hence, the beginning of the nanowire melting in this temperature region is only related to the atomic diffusion, mobility and relative rotations of shell happen, while no surface evaporation occurs. As shown in Fig 3, intensive diffusion are observed at higher temperature $T=1050$ K. In that temperature, some atomic evaporation is also found along wire axis, implying that the nanowire becomes liquidlike states. It is very interesting to observe the structural transformation of the nanowire at 1050 K. Besides the enhanced evaporation along wire axis, the helical structure of the nanowire is broken, the atomic arrangements of the nanowire have transformed from cylindrical helical to bulklike rectangular. Similar structural transition has also been observed in the size evolution of gold nanowire optimized structures in our previous simulation.[14] In the further melting process, the structures of nanowire remain bulklike. Up to 1150 K, the overall melting occurs and the structure becomes completely

disordered. Therefore, we conclude that structural transition is prior to the overall melting of the titanium nanowires. It is worth to point out that the melting behavior of titanium nanowires is different from the case of multishell gold nanowires,[12,22] where MD simulations indicate that melting starts from the interior atoms and the surface melting happens at relatively higher temperature.

From the above results and discussions, we can make the following conclusions. (1) The thermal stability of titanium nanowires significantly depends on the structures and sizes of nanowire. (2) The melting temperature of titanium nanowire is lower than the bulk's, but higher than titanium cluster's with the comparable size. (3) The coexistence mechanism of the solid state and the liquid state due to finite-size effect plays a significant role in the melting process of the thinner nanowires ($D<1.2$ nm). (4) For the thicker nanowires, i.e., $D\sim1.7$ nm, we find the structural transformation from the helical multishell cylindrical to the bulklike during the melting process. The structural transition is prior to the overall melting of the titanium nanowires.

B.L.W. and G.H.W. would like to thank financial support from National Nature Science Foundation of China (Grant No. 29890210, 10023001). J.J.Z. acknowledges support from University Research Council of University of North Carolina at Chapel Hill. X.S.C. acknowledges financial support from the Chinese National Key Basic Research Special Fund (Grant No. 2001CB610407) and from The One-hundred-person project of Chinese Academy of Sciences (Grant No. 200012).

*Email address: hyblwang@pub.hy.jsinfo.net
†Current address: Institute for Shock Physics, Washington State University, P.O. Box 642816, Pullman, Washington 99164-2816. Electronic mail address: jzhao@wsu.edu

[1] W.S. Yun, J. Kim, K.H. Park, J.S. Ha, Y.J. Ko, K. Park, S.K. Kim, Y.J. Doh, H.J. Lee, J.P. Salvetat, and L. Forro, J. Vac. Sci. Technol. A **18**, 1329 (2000).
[2] Y. Kondo and K. Takayanagi, Phys. Rev. Lett. **79**, 3455 (1997).
[3] Y. Kondo and K. Takayanagi, Science (Washington, DC, U.S.) **289**, 606 (2000); Y. Oshima, H. Koirumi, K. Mouri, H. Hirayama, K. Takayanagi, and Y. Kondo, Phys. Rev. B **65**, 121401 (2002).
[4] L. Lisiecki, A. Filankembo, H. Sack-Kongehl, K. Weiss, M.-P. Pileni, and J. Urban, Phys. Rev. B **61**, 4968 (2000).
[5] K.B. Lee, S.M. Lee, and J. Cheon, Adv. Mater. (Weinheim, Ger.) **13**, 517 (2001).
[6] B.H. Hong, S.C. Bae, C.W. Lee, S. Jeong, and K.S. Kim, Science (Washington, DC, U.S.) **294**, 348 (2001).
[7] O. Gulseren, F. Ercolessi, and E. Tosatti, Phys. Rev. B **51**, 7377 (1995).
[8] O. Gulseren, F. Ercolessi, and E. Tosatti, Phys. Rev. Lett. **80**, 3775 (1998).
[9] F. Di Tolla, A. Dal Corso, J.A. Torres, and E. Tosatti, Surf. Sci. **456**, 947 (2000).
[10] E. Tosatti, S. Prestipino, S. Kostlmeier, A. Dal Corso, and F.D. Di Tolla, Science (Washington, DC, U.S.) **291**, 288 (2001).
[11] G. Bilalbegovic, Phys. Rev. B **58**, 15 412 (1998).
[12] G. Bilalbegovic, Solid State Commun. **115**, 73 (2000).
[13] G. Bilalbegovic, J. Phys.: Condens. Matter **13**, 11531 (2001).
[14] B.L. Wang, S.Y. Yin, G.H. Wang, A. Buldum, and J.J. Zhao, Phys. Rev. Lett. **86**, 2046 (2001).
[15] B.L. Wang, S.Y. Yin, G.H. Wang, and J.J. Zhao, J. Phys.: Condens. Matter **13**, L403 (2001).
[16] B.L. Wang, G.H. Wang, and J.J. Zhao, Phys. Rev. B **65**, 235406 (2002).
[17] G.M. Finbow, R.M. Lynden-Bell, and I.R. McDonald, Mol. Phys. **92**, 705 (1997).
[18] H. Ikeda *et al.*, Phys. Rev. Lett. **82**, 2900 (1999).
[19] G. Bilalbegovic, Comput. Mater. Sci. **18**, 333 (2000).
[20] P.S. Brancio and J.P. Rino, Phys. Rev. B **62**, 16 950 (2000).
[21] J.W. Kang and H.J. Hwang, J. Phys.: Condens. Matter **14**, 2629 (2002).
[22] J.L. Wang, X.S. Chen, G.H. Wang, B.L. Wang, W. Lu, and J.J. Zhao, Phys. Rev. B **66**, 085408 (2002).
[23] Y. Imry and D.J. Scalapino, Phys. Rev. A **9**, 1672 (1974).
[24] Y. Imry, Phys. Rev. B **21**, 2042 (1980).
[25] J. Jellinek, T.L. Beck, and R.S. Berry, J. Chem. Phys. **84**, 2783 (1986); T.L. Beck, J. Jellinek, and R.S. Berry, *ibid.* **87**, 545 (1987).
[26] P. Labastie and R.L. Whetten, Phys. Rev. Lett. **65**, 1567 (1990).
[27] D.J. Wales and R.S. Berry, Phys. Rev. Lett. **73**, 2875 (1994).
[28] F. Cleri and V. Rosato, Phys. Rev. B **48**, 22 (1993).
[29] W. Hoover, Phys. Rev. A **31**, 1695 (1985).
[30] J.L. Wang, G.H. Wang, F. Ding, H. Lee, W.F. Shen, and J.J. Zhao, Chem. Phys. Lett. **341**, 529 (2001); J.L. Wang, J.J. Zhao, F. Ding, W.F. Shen, H. Lee, and G.H. Wang, Solid State Commun. **117**, 593 (2001).
[31] J.L. Wang, F. Ding, W.F. Shen, X.T. Li, G.H. Wang, and J.J. Zhao, Solid State Commun. **119**, 13 (2001).
[32] J.J. Zhao, Q. Qiu, B.L. Wang, and G.H. Wang, Solid State Commun. **118**, 157 (2001).
[33] P. Pawlow, Z. Phys. Chem., Stoechiom. Verwandtschaftsl. **65**, 545 (1909).
[34] J.P. Borel, Surf. Sci. **106**, 1 (1981).
[35] T.P. Martin, Phys. Rep. **273**, 201 (1996).